J Appl Physiol 113: 1154–1161, 2012.
First published August 16, 2012; doi:10.1152/japplphysiol.01630.2011.

HIGHLIGHTED TOPIC | *Imaging Lung Physiology*

Spatial and temporal heterogeneity of regional lung ventilation determined by electrical impedance tomography during pulmonary function testing

Barbara Vogt,[1] Sven Pulletz,[1] Gunnar Elke,[1] Zhanqi Zhao,[2] Peter Zabel,[3] Norbert Weiler,[1] and Inéz Frerichs[1]

[1]*Department of Anesthesiology and Intensive Care Medicine, University Medical Center Schleswig-Holstein, Campus Kiel, Kiel, Germany;* [2]*Department of Biomedical Engineering, Furtwangen University, Villingen-Schwenningen, Germany; and* [3]*Department of Pneumology, Medical Clinic, Research Center Borstel, Borstel, Germany*

Submitted 3 January 2012; accepted in final form 8 August 2012

Vogt B, Pulletz S, Elke G, Zhao Z, Zabel P, Weiler N, Frerichs I. Spatial and temporal heterogeneity of regional lung ventilation determined by electrical impedance tomography during pulmonary function testing. *J Appl Physiol* 113: 1154–1161, 2012. First published August 16, 2012; doi:10.1152/japplphysiol.01630.2011.— Electrical impedance tomography (EIT) is a functional imaging modality capable of tracing continuously regional pulmonary gas volume changes. The aim of our study was to determine if EIT was able to assess spatial and temporal heterogeneity of ventilation during pulmonary function testing in 14 young (37 ± 10 yr, mean age ± SD) and 12 elderly (71 ± 9 yr) subjects without lung disease and in 33 patients with chronic obstructive pulmonary disease (71 ± 9 yr). EIT and spirometry examinations were performed during tidal breathing and a forced vital capacity (FVC) maneuver preceded by full inspiration to total lung capacity. Regional inspiratory vital capacity (IVC); FVC; forced expiratory volume in 1 s (FEV_1); FEV_1/FVC; times required to expire 25%, 50%, 75%, and 90% of FVC (t_{25}, t_{50}, t_{75}, t_{90}); and tidal volume (V_T) were determined in 912 EIT image pixels in the chest cross section. Coefficients of variation (CV) were calculated from all pixel values of IVC, FVC, FEV_1, and V_T to characterize the ventilation heterogeneity. The highest values were found in patients, and no differences existed between the healthy young and elderly subjects. Receiver-operating characteristics curves showed that CV of regional IVC, FVC, FEV_1, and V_T discriminated the young and elderly subjects from the patients. Frequency distributions of pixel FEV_1/FVC, t_{25}, t_{50}, t_{75}, and t_{90} identified the highest ventilation heterogeneity in patients but distinguished also the healthy young from the elderly subjects. These results indicate that EIT may provide additional information during pulmonary function testing and identify pathologic and age-related spatial and temporal heterogeneity of regional lung function.

EIT; ventilation distribution; ventilation homogeneity; regional lung function; COPD

ELECTRICAL IMPEDANCE TOMOGRAPHY (EIT) is a functional radiation-free imaging modality. Its measuring principle is based on the measurement of electrical bioimpedance using an array of electrodes placed on the circumference of the studied body section. Since the invention of EIT, thoracic EIT examinations have been considered to possess the highest potential for clinical use. This is related to the fact that physiological lung ventilation (17, 39, 41), mechanical lung ventilation (13, 36, 53), and lung diseases (26, 33, 50) affect the electrical properties of lung tissue.

Regional ventilation-related changes in lung aeration periodically modify regional electrical current conduction pathways. The resulting changes in electrical lung tissue impedance are proportional to regional changes in gas content. This was confirmed in multiple EIT validation studies using other established imaging modalities such as computed tomography (49, 51), electron-beam computed tomography (19), positron emission tomography (40), single-photon emission computed tomography (23), and ventilation scintigraphy (25, 46) or other medical examination techniques such as spirometry (1, 18, 21) or multiple-breath nitrogen washout (22).

The development of EIT technology toward a clinical examination tool was mainly driven by this capability of EIT to continuously detect regional lung ventilation at the bedside at very high scan rates without exposing the patients to radiation. It was realized that these advantageous features of EIT might be beneficial for monitoring regional lung ventilation in mechanically ventilated patients. Because EIT is able to detect regional lung overdistension, atelectasis, recruitment, and derecruitment (11, 13, 29, 31, 50) it might become a useful tool to provide rapid feedback on the regional effects of changed ventilator settings. This information could potentially be used to minimize the injurious effects of mechanical ventilation.

However, EIT may provide valuable diagnostic information in other, spontaneously breathing patients as well. EIT could facilitate early diagnosis and initiation of therapy in patients with latent lung diseases of heterogeneous nature not detected by conventional examination methods. For instance, standard pulmonary function testing by spirometry or whole body plethysmography need not reveal the heterogeneity of regional lung function because it cannot be identified from the global signal sampled at the airway opening. Patients with manifest diseases might also benefit from EIT. Natural disease progression and response to treatment could be assessed by EIT monitoring.

Therefore, we initiated a study with the aim of checking if EIT was able to identify nonhomogeneous regional lung ventilation in patients with existing obstructive lung disease in comparison with healthy subjects with no history of lung disease. To account for age-dependent changes in regional lung function, we studied both young and elderly healthy adults. We performed the examinations during pulmonary function testing using well-established ventilation maneuvers and during spon-

Address for reprint requests and other correspondence: I. Frerichs, Dept. of Anesthesiology and Intensive Care Medicine, Univ. Medical Center Schleswig-Holstein, Campus Kiel, Arnold-Heller Str. 3, D-24105 Kiel, Germany (e-mail: frerichs@anaesthesie.uni-kiel.de).

Table 1. *Physical characteristics of all studied subjects*

Subjects	Age, yr	Sex		Height, cm	Weight, kg
		M	F		
Young	37 ± 10	6	8	176 ± 9	71 ± 11
Elderly	71 ± 9	10	1	175 ± 7	85 ± 12
COPD	71 ± 9	20	13	171 ± 9	75 ± 19

Values are means ± SD. COPD, chronic obstructive pulmonary disease; M, male; F, female.

taneous tidal breathing and examined if EIT-derived measures of spatial and temporal lung function heterogeneity were able to discriminate the patients from healthy subjects.

MATERIALS AND METHODS

Subjects and examination protocol. We examined three groups of subjects of both sexes: *1*) 14 young healthy adults with no history of lung disease, *2*) 12 elderly healthy subjects with no history of lung disease, and *3*) 33 patients with chronic obstructive pulmonary disease (COPD). Physical characteristics of the studied subjects and pulmonary function data are given in Tables 1 and 2, respectively. All subjects from the first two groups were nonsmokers. With the exception of two patients, all subjects in the third group were smokers or former smokers with 10 to 100 pack years. Six patients were classified as GOLD (Global Initiative for Chronic Obstructive Lung Disease) stage II, nine as stage III, and 18 as stage IV. All patients received long-term bronchodilator therapy; in 27 patients corticosteroids were additionally administered. Thirty patients exhibited emphysematous changes in chest radiography; in 17 of these patients bronchiectasies were identified. Bullous emphysema was not documented in any of the patients. The study was approved by the institutional ethics committee, and written informed consent was obtained from each subject.

Sixteen self-adhesive electrodes (Blue Sensor L-00-S, Ambu, Ballerup, Denmark or RedDot, 3M Medica, St. Paul, MN) were placed on the chest circumference in the 5–6th intercostal space (parasternal line) and one reference electrode on the abdomen in each subject. All subjects were examined by electrical impedance tomography (Goe-MF II EIT system, CareFusion, Höchberg, Germany) and spirometry (Jaeger pneumotachograph, CareFusion, Höchberg, Germany) in a seated position during spontaneous tidal breathing and subsequent full inspiration from residual volume to total lung capacity followed by standard forced full expiration maneuver.

EIT data acquisition and analysis. EIT examinations were performed using electrical excitation currents of 5 mA_{rms} and 50 kHz. Adjacent electrode current drive and voltage measurement pattern was used. This means that 16 consecutive current injections were performed during each measuring cycle. The resulting voltages were measured by 13 passive adjacent electrode pairs during each of these current injections. (The active electrode pair and the pairs next to it were excluded from voltage measurement.) Two hundred eight (16 × 13) voltages were acquired during each cycle. EIT scans were generated from these raw data using the weighted back-projection algorithm at a rate of up to 44 scans/s. Nine hundred twelve image pixels (a circular area within a square grid of 32 × 32 pixels) contained the EIT data. Each image pixel of an individual EIT scan showed the difference between the instantaneous (Z) and reference pixel impedance (Z_{ref}) normalized by Z_{ref}, i.e., $(Z\text{-}Z_{ref})/Z_{ref}$. In EIT publications, this value is often called relative impedance change (rel. ΔZ), and this term is also used in the following text. Individual pixel Z_{ref} was defined as average pixel Z during the period of quiet tidal breathing. Data acquisition lasted ~60–100 s and was terminated after the full forced expiration maneuver. More details on EIT data acquisition and image reconstruction can be found elsewhere (6, 9, 42).

Further EIT data analysis was performed offline. At first, a period of quiet tidal breathing comprising four to six breaths was identified in the pixel tracings of rel. ΔZ. Average tidal amplitude of rel. ΔZ was then calculated in each image pixel by identifying the inspiratory maxima and expiratory minima of the signal. This value quantified the average pixel tidal volume (V_T) during the analyzed period of tidal breathing. Afterward, other relevant time points were identified: the start and end points of the full inspiration maneuver at residual lung volume and total lung capacity, respectively, the onset of the forced full expiration and its end, as well as the time point exactly 1 s after the beginning of the forced expiration. The pixel values of rel. ΔZ at these time points were used to calculate the pixel impedance differences between *1*) residual lung volume and total lung capacity after full inspiration, corresponding to inspiratory vital capacity (IVC), *2*) total lung capacity and lung volume after 1 s of forced expiration, corresponding to forced expiratory volume in one second (FEV_1), and *3*) total lung capacity and the lung volume by the end of the forced full expiration, corresponding to forced vital capacity (FVC). Finally, the times required to exhale 25% (t_{25}), 50% (t_{50}), 75% (t_{75}), and 90% (t_{90}) of pixel FVC were determined from each pixel tracing of rel. ΔZ.

The 912 pixel values of IVC, FEV_1, FVC, and V_T calculated from the EIT data in each studied subject were further processed as follows. First, functional EIT scans showing the distribution of regional IVC, FEV_1, FVC, and V_T in the chest cross section were generated. Afterward, mean values of IVC, FEV_1, FVC, and V_T were calculated. These values served as a measure of regional IVC, FEV_1, FVC, and V_T in the studied section of the chest and they were compared with the global volumes measured by spirometry. Finally, standard deviations of all pixel values of IVC, FEV_1, FVC, and V_T were determined and coefficients of variation (CV) were calculated as the ratios of standard deviations to the corresponding mean values. CV values of regional IVC, FEV_1, FVC, and V_T were used to characterize the heterogeneity of their spatial distribution in the chest cross section. Mean and CV values were compared among the three studied groups. Receiver-operating characteristics (ROC) analysis was used to characterize the power of CV of all four EIT-derived regional lung volumes to discriminate between the patients and healthy subjects based on the calculation of the areas under the ROC curves.

To further characterize the spatial and also temporal distribution of regional lung ventilation, frequency distributions of pixel FEV_1/FVC and pixel t_{25}, t_{50}, t_{75}, and t_{90} were calculated and presented as histograms.

Statistical analysis. Statistical analysis was performed with GraphPad Prism version 5.01 (GraphPad Software, San Diego, CA). One-way analysis of variance with Bonferroni post test was used to test the significance of differences in mean and CV values of regional IVC,

Table 2. *Lung function data of all studied subjects*

Subjects	FEV_1, liters (% predicted)	FVC, liters (% predicted)	FEV_1/FVC (% predicted)	PEF liters/s (% predicted)
Young	3.96 ± 1.06 (107.1 ± 14.0)	4.6 ± 1.18 (105.3 ± 16.0)	0.86 ± 0.08 (103.9 ± 8.8)	8.32 ± 1.91 (101.7 ± 19.8)
Elderly	3.23 ± 0.90 (104.8 ± 18.0)	4.06 ± 1.00 (99.6 ± 19.3)	0.79 ± 0.06 (106.9 ± 16.6)	6.77 ± 1.93 (86.3 ± 23.4)
COPD	1.06 ± 0.41 (41.6 ± 15.9)	2.14 ± 0.67 (66.0 ± 18.1)	0.50 ± 0.11 (64.1 ± 15.1)	2.27 ± 1.11 (32.7 ± 14.4)

Values are means ± SD. FEV_1, forced expiratory volume in 1 s; FVC, forced vital capacity; PEF, peak expiratory flow; % predicted, percent of values predicted according to the European Respiratory Society.

FEV_1, FVC, and V_T among the three studied groups. Additional analysis with included COPD subgroups based on the GOLD classification was performed. ROC curves were generated to compare the predictive power of CV of regional IVC, FEV_1, FVC, and V_T in distinguishing the COPD patients from healthy young and elderly subjects. Correlation between regional and global volumes was quantified by the coefficient of determination (r^2). P values <0.05 were considered significant.

RESULTS

The quantitative analysis of all studied subjects (Fig. 1) revealed that regional IVC, FEV_1, and FVC determined by EIT in the young healthy subjects were significantly higher than in the elderly healthy subjects. The COPD patients exhibited significantly lower values than both the young and the elderly. Regional V_T was higher in the young subjects, but the elderly and the COPD patients did not significantly differ from each other. Regional lung volumes determined by EIT correlated with global spirometric volumes. The following r^2 values were determined in the young healthy subjects [0.986 ± 0.011 (mean ± SD)], in the elderly (0.962 ± 0.051), and in the COPD patients (0.877 ± 0.148).

CV of regional IVC, FEV_1, FVC, and V_T as an aggregate measure of ventilation heterogeneity showed no significant differences between the healthy young and elderly subjects (Fig. 2). The corresponding CV values were significantly higher in the COPD patients than in both groups of healthy subjects and exhibited higher variation. With GOLD stage-based subgroup analysis, significant differences in CV of regional IVC, FVC, and V_T were found between the GOLD stage IV patients and healthy young and elderly subjects, respectively.

The generated ROC curves showing the power of CV of regional IVC, FEV_1, FVC, and V_T to discriminate between the COPD patients and the young and elderly subjects, respectively, are presented in Fig. 3. (The CV values did not distinguish the young from the elderly subjects and the corresponding ROC curves were close to the line of identity and are not plotted in the diagrams of Fig. 3.) The presented ROC curves indicate that the CV values of all EIT-derived regional lung volumes had the power to significantly discriminate between the patients and the healthy subjects. The only exception was the CV of regional IVC, which showed only a trend in distinguishing the COPD patients from the elderly ($P = 0.060$). CV of regional FEV_1 exhibited the highest discriminating power, but even the CV values obtained from quiet tidal breathing were able to significantly distinguish between the healthy subjects and patients.

The histograms of pixel FEV_1/FVC values identified the dissimilar frequency distribution patterns of this measure among all three groups (Fig. 4). As expected, the young healthy subjects had the highest values of pixel FEV_1/FVC ratios with a narrow peak in the distribution histogram. In the elderly, the values were shifted to the left with a broader peak. The highest degree of heterogeneity with a flat distribution pattern in the histogram was noted in the COPD patients.

The histograms of pixel t_{25}, t_{50}, t_{75}, and t_{90} (Fig. 5) revealed the lowest temporal heterogeneity of regional lung emptying in the young healthy subjects. Compared with the young group, the elderly exhibited slower emptying (the pixel t_{25}, t_{50}, t_{75}, and t_{90} values were shifted to the right) and a higher degree of temporal heterogeneity in lung emptying. In the COPD patients, delayed and more heterogeneous emptying

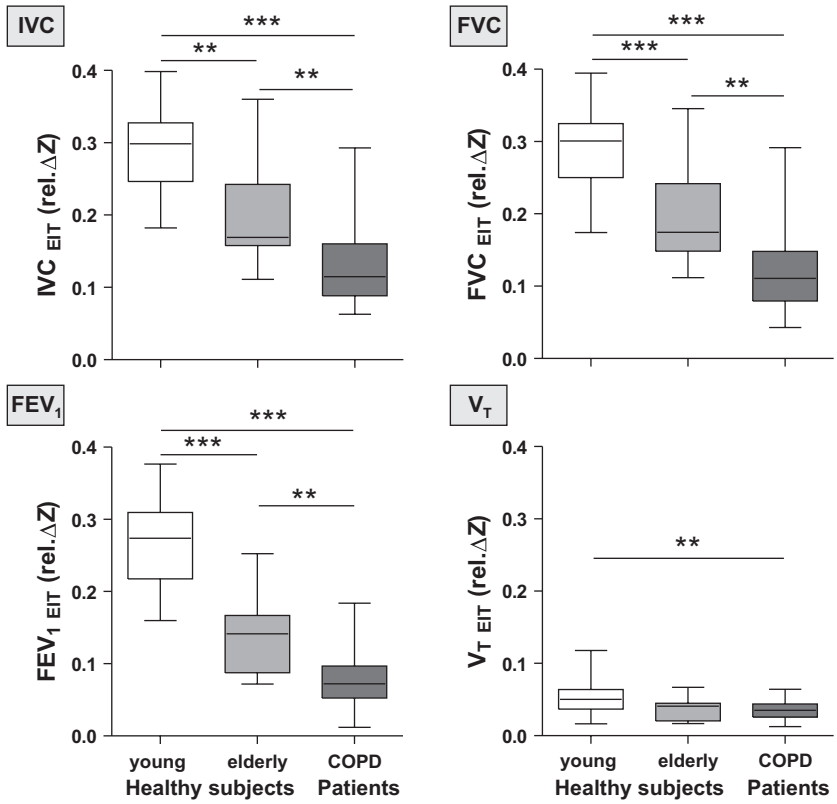

Fig. 1. Average relative impedance change (rel. ΔZ) in the examined chest cross section reflecting regional inspiratory vital capacity (IVC; *top left*), forced expiratory volume in 1 s (FEV_1; *bottom left*), forced vital capacity (FVC; *top right*), and tidal volume (V_T; *bottom right*) determined by electrical impedance tomography (EIT) in healthy young and elderly adults and patients with chronic obstructive pulmonary disease (COPD). Box and whisker plots show the minimum, 25% percentile, median, 75% percentile, and maximum values. Significant differences among the groups are indicated: $^{**}P < 0.01$; $^{***}P < 0.001$.

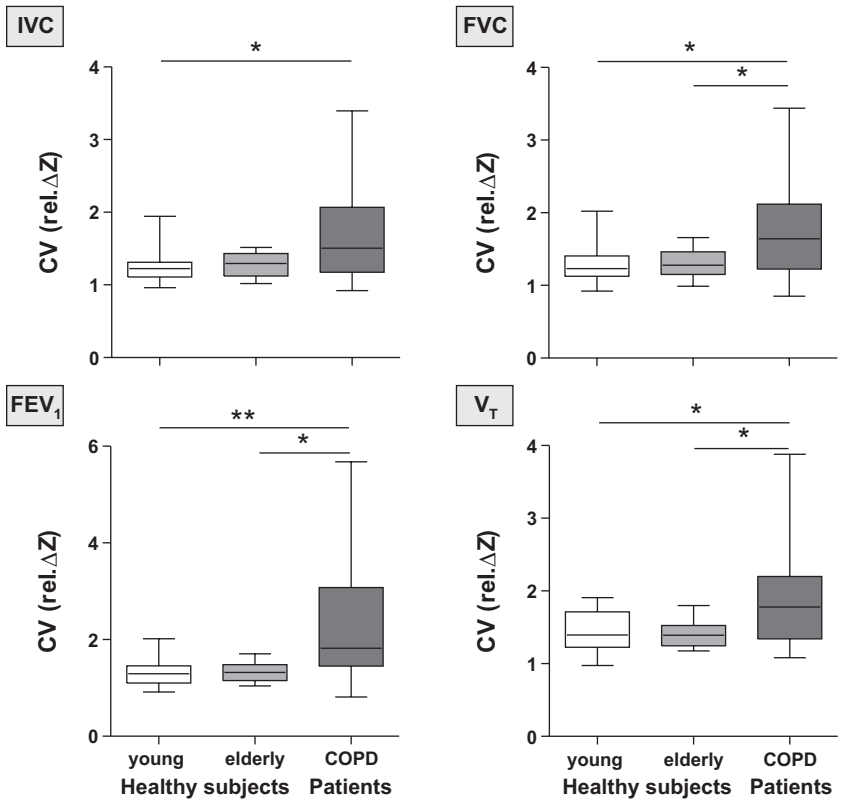

Fig. 2. Coefficient of variation (CV) of regional IVC (*top left*), FEV_1 (*bottom left*), FVC (*top right*), and V_T (*bottom right*) in the chest cross section determined by EIT in healthy young and elderly adults and COPD patients. Box and whisker plots show the minimum, 25% percentile, median, 75% percentile, and maximum values. Significant differences among the groups are indicated: $*P < 0.05$; $**P < 0.01$.

than in the healthy subjects was noted already after the exhalation of 25% of FVC and the frequency distribution became flat after the exhalation of 75% of FVC.

DISCUSSION

The results of our study showed that EIT was able to assess the distribution of regional IVC, FEV_1, FVC, and V_T in the chest cross section of healthy young and elderly subjects and patients with COPD. Regional IVC, FEV_1, FVC, and V_T exhibited significant differences among the three groups with the lowest values found in the patients corresponding to the global volumes determined by spirometry. CV of EIT-derived regional IVC, FEV_1, FVC, and V_T identified the most heterogeneous distribution of ventilation in the COPD patients. However, this gross measure of spatial heterogeneity showed no differences in the degree of ventilation heterogeneity between the young and elderly subjects with no lung disease. The frequency distributions of pixel FEV_1/FVC and pixel t_{25}, t_{50}, t_{75}, and t_{90} revealed the differences in spatial and temporal ventilation distribution not only between the COPD patients and the young and elderly healthy subjects, respectively, but also between the two age groups of healthy subjects.

EIT was already often applied to determine ventilation distribution in experimental and clinical studies, usually during spontaneous tidal breathing or during mechanical ventilation using various ventilator modes and maneuvers. EIT examinations during pulmonary function testing are rare. In the former studies, ventilation distribution was usually quantified using regions of interest (ROI). The typical ROIs were right or left hemithoraces, anterior or posterior halves of the scans, image quadrants, three to four anteroposterior layers (13, 30, 32, 37, 47, 49), or anteroposterior ventilation profiles (5, 16). The latter two approaches were reasonable when supine subjects were examined by EIT because they allowed the assessment of differences in ventilation between the dependent and nondependent lung regions.

In seated subjects, like in our study, the EIT electrode plane is perpendicular with the gravity vector. Thus the effect of gravity is comparable within the examined chest plane. For this reason and also because we wanted to exploit all available regional data, we quantified the spatial heterogeneity of lung ventilation by EIT using measures of ventilation distribution based on all pixel values of EIT-derived lung volumes. We determined CV of four different regional lung volumes as an aggregate measure of ventilation heterogeneity because this measure was previously applied in studies aiming to quantify the spatial variation in ventilation distribution using other examination techniques (8, 43, 52). A similar approach to calculate an index of ventilation inhomogeneity was recently suggested (53). In addition, we determined the frequency distributions of pixel FEV_1/FVC. We chose these values because the ratio of global FEV_1 and FVC is an established measure characterizing airflow limitation in conventional pulmonary function testing.

By using these measures, EIT found the highest degree of spatial ventilation heterogeneity in COPD patients when compared with the healthy young but also with the elderly subjects of comparable age. This higher heterogeneity was detected during all analyzed phases of dynamically acquired data during deep inspiration, forced expiration, and spontaneous tidal breathing. This corresponds to previous findings obtained, e.g., by hyperpolarized ^{3}He-magnetic resonance imaging (14, 48), show-

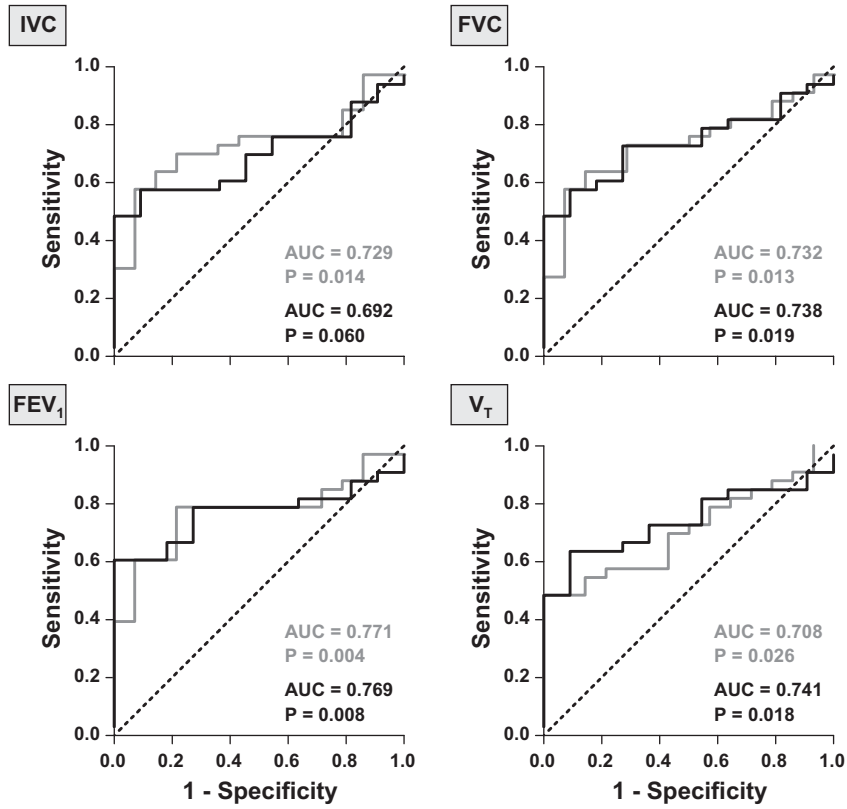

Fig. 3. Receiver-operating characteristics (ROC) curves indicating the power of CV of regional IVC (*top left*), FEV_1 (*bottom left*), FVC (*top right*), and V_T (*bottom right*) to discriminate between patients with COPD and the young (shaded lines) and elderly subjects (solid lines) with no lung disease, respectively. Line of identity (dashed line) and *P* values are given in each diagram. AUC, area under the curve.

ing that topographical distribution of ventilation was affected by the underlying lung pathology in COPD patients and less homogeneous than in normal subjects.

ROC analysis revealed the ability of CV of regional IVC, FEV_1, FVC, and V_T to significantly discriminate COPD patients from the young and elderly subjects with no lung disease. Because airway obstruction becomes most manifest and affects regional ventilation mainly during forced expiration, CV of regional FEV_1 exhibited the highest discriminating power. The possibility to distinguish the COPD patients from the healthy subjects even during quiet breathing without the necessity to perform the standard forced full expiration maneuver is an interesting finding because it is known that this maneuver is highly dependent on patient cooperation and effort.

We did not find any differences in ventilation heterogeneity quantified by the CV values between the young and elderly subjects, although regional IVC, FEV_1, and FVC were significantly lower in the aged subjects as expected (44). Ventilation deficits may exist in the elderly, even if they have no history of lung disease or smoking (34). The reason why the CV values of pixel EIT lung volumes did not detect such small ventilation deficits in our study could be the low sensitivity of this measure. In fact, the more sophisticated analyses using the frequency distributions of pixel FEV_1/FVC and pixel t_{25}, t_{50}, t_{75}, and t_{90} identified the dissimilarities in spatial and also temporal ventilation distribution between the two age groups of healthy subjects. It also has to be pointed out that, in contrast with the studies using conventional imaging modalities, our patients were examined in an upright and not in a supine posture. It is known that the dependent lung regions are prone to earlier airway closure on expiration in older than in younger adults (24, 27). This early airway closure was already found by

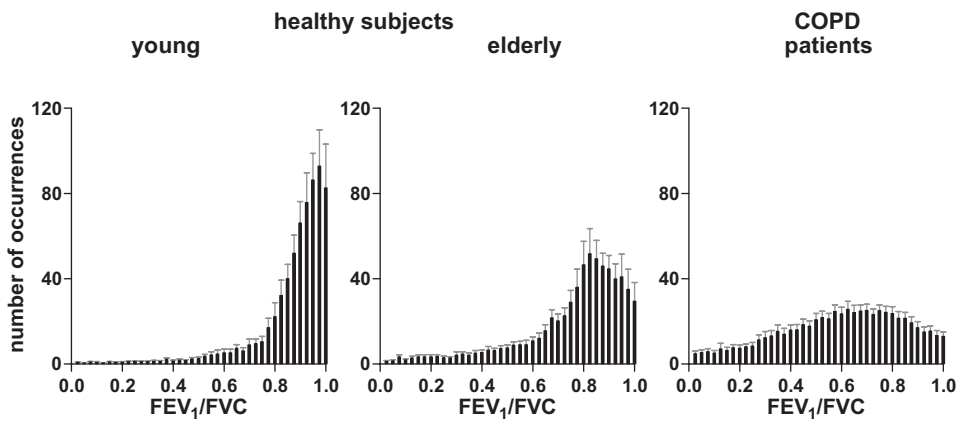

Fig. 4. Frequency distributions of pixel FEV_1/FVC ratios in the young (*left*) and elderly subjects (*middle*) with no lung disease and in patients with COPD (*right*). Histograms show mean values ± SE.

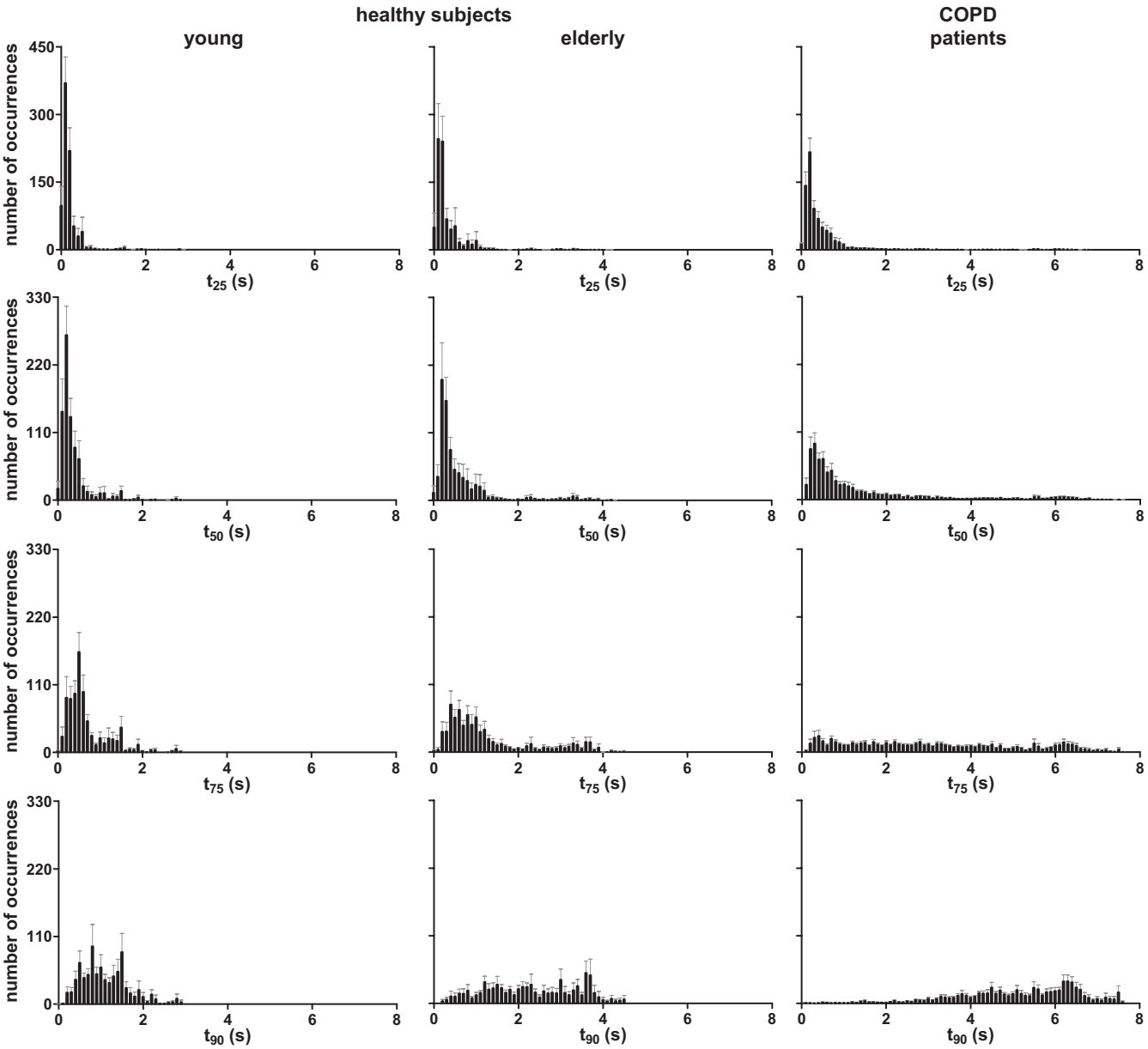

Fig. 5. Frequency distributions of pixel times required to exhale 25% (t_{25}), 50% (t_{50}), 75% (t_{75}), and 90% (t_{90}) of pixel FVC in the young (*left*) and elderly subjects (*middle*) with no lung disease and in patients with COPD (*right*). Histograms show mean values ± SE.

EIT in the elderly in recumbent postures (15); therefore, the dissimilar spatial and temporal distribution of regional lung ventilation between the young and elderly subjects might be enhanced in other than in the upright posture.

Additional measures could be generated from regional EIT data obtained during pulmonary function testing in the future, for instance from pixel flow-volume curves. Such measures may enhance the capability of EIT to detect ventilation heterogeneity and to discriminate among various degrees of lung function compromise. However, the current EIT sampling rates are still lower when compared with pneumotachography with the consequence that, especially during very fast flow rates, only few data points are sampled. In addition, regional EIT signals are slightly affected by the cardiac and lung perfusion-related changes in electrical impedance that become discernible especially at low air flow rates.

Limitations. Compared with other imaging modalities, the spatial resolution of EIT scans is low and its ability to assess lung morphology is limited. However, the strength of EIT is that it allows functional lung imaging. Compared with conventional imaging modalities such as chest radiography and computed tomography where the corresponding images are typically obtained during breath-hold, EIT scanning can be performed during tidal breathing and/or ventilation maneuvers. As shown by the current results, EIT data acquired at scan rates exceeding by far those of other imaging modalities enable the assessment of regional lung function in a total of 912 image pixels in the chest cross section.

The fact that EIT scanning is typically performed only in one transverse chest plane could be considered another limitation. However, EIT scans also reflect out-of-plane impedance changes because electrical current pathways are not confined to

a single plane (38). Therefore, regional lung function can be analyzed not just in a two-dimensional plane but from a rather large slice of the lung tissue extending several centimeters above and below the level where the electrodes are placed (20). It was previously determined that the electrode plane influenced the EIT findings in healthy subjects (39), therefore, we always placed the electrodes in the 5–6th intercostal space in all subjects and patients in our study. The effect of electrode plane has never been studied in COPD patients so it remains to be established whether the specific characteristics of COPD, such as the barrel chest, impact the EIT data.

At present, the majority of EIT devices, including the device used in our study, uses the adjacent current drive and voltage measurement pattern. This approach exhibits several disadvantages (3, 42, 45). Further technological development of EIT hardware may improve the performance of the devices and increase the data quality.

In our study, EIT scans were reconstructed using the filtered back-projection, which is one of the oldest image reconstruction algorithms (7). It was applied in most of the experimental and clinical EIT studies performed up to now. Its suitability to track regional changes in physiological lung functions was validated (35). Nevertheless, other reconstruction algorithms may improve the image quality because they offer several theoretical advantages (2, 28). Implementation of a priori anatomical information may also be of benefit (28).

Finally, a certain limitation of the present study is that we included patients without attempting to differentiate among different pathological pathways leading to COPD. COPD is a very heterogeneous disease (4). Its definition is based on the finding of irreversible airflow limitation. Consequently, patients of different phenotypes were pooled in our COPD group, precluding meaningful subanalysis. This explains why significant differences were only identified between the GOLD IV stage patients and the young and the elderly healthy subjects, respectively. This finding is understandable because the staging of patients based solely on global FEV_1 and FEV_1/FVC is too simple to reflect the complexity of the disease (10) and because the severity of disease is not a phenotype (4). Despite this last study limitation, the results of our study document the feasibility of EIT to determine the distribution of regional ventilation and its ability to establish pathologically induced and age-related changes in regional lung function.

Perspectives. There exist general and specific features of EIT that delineate its clinical perspectives in regional pulmonary function testing. The major general advantages of EIT are the high scan rates, no need of radiation exposure, and portability. The patients need not to be transferred to special examination sites, and they can be repeatedly examined because there are no known hazards associated with EIT use. EIT examinations can be accomplished during dynamic conditions.

The current findings showed that EIT was able to assess standard pulmonary function measures on a regional lung level and that advanced analysis of EIT data generated new functional measures of spatial and temporal ventilation heterogeneity. These measures identified the higher degree of ventilation heterogeneity in the COPD patients compared with the healthy subjects, even of similar age. Therefore, EIT might become useful in screening for detection of early stages of COPD (and possibly of other lung diseases). EIT could also be utilized in later monitoring of disease progression and therapy (e.g., bronchodilator therapy) in addition to already established clinical imaging techniques (12) and standard pulmonary function testing by spirometry and whole body plethysmography. Along with other clinical, functional, and imaging data EIT might be applied to precisely characterize COPD phenotypically. Further studies will be needed to provide the evidence.

Conclusion

Our study showed that EIT was able to assess spatial and temporal distribution of different regional lung volumes during spontaneous tidal breathing and forced ventilation maneuvers and identify not only pathologically induced but even the less pronounced age-related increase in ventilation heterogeneity. The EIT-derived measures of regional lung function might become useful in a clinical setting, providing complementary information to already established examination tools.

GRANTS

The Medical Faculty of the Christian Albrechts University in Kiel, Germany has supported B. Vogt as clinical researcher by funding a 1-yr rotational position.

DISCLOSURES

No conflicts of interest, financial or otherwise, are declared by the authors.

AUTHOR CONTRIBUTIONS

Author contributions: B.V., P.Z., N.W., and I.F. conception and design of research; B.V., S.P., G.E., and I.F. performed experiments; B.V., Z.Z., and I.F. analyzed data; B.V., N.W., and I.F. interpreted results of experiments; B.V. and I.F. drafted manuscript; B.V., S.P., G.E., P.Z., N.W., and I.F. edited and revised manuscript; B.V., S.P., G.E., Z.Z., P.Z., N.W., and I.F. approved final version of manuscript; I.F. prepared figures.

REFERENCES

1. **Adler A, Amyot R, Guardo R, Bates JH, Berthiaume Y.** Monitoring changes in lung air and liquid volumes with electrical impedance tomography. *J Appl Physiol* 83: 1762–1767, 1997.
2. **Adler A, Arnold JH, Bayford R, Borsic A, Brown B, Dixon P, Faes TJ, Frerichs I, Gagnon H, Garber Y, Grychtol B, Hahn G, Lionheart WR, Malik A, Patterson RP, Stocks J, Tizzard A, Weiler N, Wolf GK.** GREIT: a unified approach to 2D linear EIT reconstruction of lung images. *Physiol Meas* 30: S35–55, 2009.
3. **Adler A, Gaggero PO, Maimaitijiang Y.** Adjacent stimulation and measurement patterns considered harmful. *Physiol Meas* 32: 731–744, 2011.
4. **Agusti A, Sobradillo P, Celli B.** Addressing the complexity of chronic obstructive pulmonary disease: from phenotypes and biomarkers to scale-free networks, systems biology, and P4 medicine. *Am J Respir Crit Care Med* 183: 1129–1137, 2011.
5. **Armstrong RK, Carlisle HR, Davis PG, Schibler A, Tingay DG.** Distribution of tidal ventilation during volume-targeted ventilation is variable and influenced by age in the preterm lung. *Intensive Care Med* 37: 839–846, 2011.
6. **Barber D, Brown B.** Applied potential tomography. *J Phys E Sci Instrum* 17: 723–733, 1984.
7. **Barber DC, Seagar AD.** Fast reconstruction of resistance images. *Clin Phys Physiol Meas* 8, *Suppl* A: 47–54, 1987.
8. **Bayat S, Porra L, Suhonen H, Suortti P, Sovijarvi AR.** Paradoxical conducting airway responses and heterogeneous regional ventilation after histamine inhalation in rabbit studied by synchrotron radiation CT. *J Appl Physiol* 106: 1949–1958, 2009.
9. **Boone K, Barber D, Brown B.** Imaging with electricity: report of the European Concerted Action on Impedance Tomography. *J Med Eng Technol* 21: 201–232, 1997.
10. **Casanova C, de Torres JP, Aguirre-Jaime A, Pinto-Plata V, Marin JM, Cordoba E, Baz R, Cote C, Celli BR.** The progression of chronic obstructive pulmonary disease is heterogeneous: the experience of the BODE cohort. *Am J Respir Crit Care Med* 184: 1015–1021, 2011.
11. **Costa EL, Borges JB, Melo A, Suarez-Sipmann F, Toufen C Jr, Bohm SH, and Amato MB.** Bedside estimation of recruitable alveolar collapse

and hyperdistension by electrical impedance tomography. *Intensive Care Med* 35: 1132–1137, 2009.
12. **Coxson HO, Mayo J, Lam S, Santyr G, Parraga G, Sin DD.** New and current clinical imaging techniques to study chronic obstructive pulmonary disease. *Am J Respir Crit Care Med* 180: 588–597, 2009.
13. **Dargaville PA, Rimensberger PC, Frerichs I.** Regional tidal ventilation and compliance during a stepwise vital capacity manoeuvre. *Intensive Care Med* 36: 1953–1961, 2010.
14. **Fain S, Schiebler ML, McCormack DG, Parraga G.** Imaging of lung function using hyperpolarized helium-3 magnetic resonance imaging: review of current and emerging translational methods and applications. *J Magn Reson Imaging* 32: 1398–1408, 2010.
15. **Frerichs I, Braun P, Dudykevych T, Hahn G, Genee D, Hellige G.** Distribution of ventilation in young and elderly adults determined by electrical impedance tomography. *Respir Physiol Neurobiol* 143: 63–75, 2004.
16. **Frerichs I, Dargaville PA, van Genderingen H, Morel DR, Rimensberger PC.** Lung volume recruitment after surfactant administration modifies spatial distribution of ventilation. *Am J Respir Crit Care Med* 174: 772–779, 2006.
17. **Frerichs I, Dudykevych T, Hinz J, Bodenstein M, Hahn G, Hellige G.** Gravity effects on regional lung ventilation determined by functional EIT during parabolic flights. *J Appl Physiol* 91: 39–50, 2001.
18. **Frerichs I, Hahn G, Hellige G.** Thoracic electrical impedance tomographic measurements during volume controlled ventilation-effects of tidal volume and positive end-expiratory pressure. *IEEE Trans Med Imaging* 18: 764–773, 1999.
19. **Frerichs I, Hinz J, Herrmann P, Weisser G, Hahn G, Dudykevych T, Quintel M, Hellige G.** Detection of local lung air content by electrical impedance tomography compared with electron beam CT. *J Appl Physiol* 93: 660–666, 2002.
20. **Hahn G, Hartung C, Hellige G.** *Elektrische Impedanztomographie (EIT) als Methode zur regionalen Beurteilung der Lungenventilation*, edited by Thews G. Mainz: Gustav Fischer Verlag, 1998.
21. **Harris ND, Suggett AJ, Barber DC, Brown BH.** Applications of applied potential tomography (APT) in respiratory medicine. *Clin Phys Physiol Meas* 8, *Suppl* A: 155–165, 1987.
22. **Hinz J, Moerer O, Neumann P, Dudykevych T, Hellige G, Quintel M.** Effect of positive end-expiratory-pressure on regional ventilation in patients with acute lung injury evaluated by electrical impedance tomography. *Eur J Anaesthesiol* 22: 817–825, 2005.
23. **Hinz J, Neumann P, Dudykevych T, Andersson LG, Wrigge H, Burchardi H, Hedenstierna G.** Regional ventilation by electrical impedance tomography: a comparison with ventilation scintigraphy in pigs. *Chest* 124: 314–322, 2003.
24. **Holland J, Milic-Emili J, Macklem PT, Bates DV.** Regional distribution of pulmonary ventilation and perfusion in elderly subjects. *J Clin Invest* 47: 81–92, 1968.
25. **Kunst PW, Vonk Noordegraaf A, Hoekstra OS, Postmus PE, de Vries PM.** Ventilation and perfusion imaging by electrical impedance tomography: a comparison with radionuclide scanning. *Physiol Meas* 19: 481–490, 1998.
26. **Kunst PW, Vonk Noordegraaf A, Straver B, Aarts RA, Tesselaar CD, Postmus PE, de Vries PM.** Influences of lung parenchyma density and thoracic fluid on ventilatory EIT measurements. *Physiol Meas* 19: 27–34, 1998.
27. **Leblanc P, Ruff F, Milic-Emili J.** Effects of age and body position on "airway closure" in man. *J Appl Physiol* 28: 448–451, 1970.
28. **Lionheart WR.** EIT reconstruction algorithms: pitfalls, challenges and recent developments. *Physiol Meas* 25: 125–142, 2004.
29. **Lowhagen K, Lindgren S, Odenstedt H, Stenqvist O, Lundin S.** A new non-radiological method to assess potential lung recruitability: a pilot study in ALI patients. *Acta Anaesthesiol Scand* 55: 165–174, 2011.
30. **Lowhagen K, Lundin S, Stenqvist O.** Regional intratidal gas distribution in acute lung injury and acute respiratory distress syndrome-assessed by electric impedance tomography. *Minerva Anestesiol* 76: 1024–1035, 2010.
31. **Meier T, Luepschen H, Karsten J, Leibecke T, Grossherr M, Gehring H, Leonhardt S.** Assessment of regional lung recruitment and derecruitment during a PEEP trial based on electrical impedance tomography. *Intensive Care Med* 34: 543–550, 2008.
32. **Miedema M, de Jongh FH, Frerichs I, van Veenendaal MB, van Kaam AH.** Changes in lung volume and ventilation during surfactant treatment in ventilated preterm infants. *Am J Respir Crit Care Med* 184: 100–105, 2011.
33. **Miedema M, Frerichs I, de Jongh FH, van Veenendaal MB, van Kaam AH.** Pneumothorax in a preterm infant monitored by electrical impedance tomography: a case report. *Neonatology* 99: 10–13, 2011.
34. **Parraga G, Mathew L, Etemad-Rezai R, McCormack DG, Santyr GE.** Hyperpolarized 3He magnetic resonance imaging of ventilation defects in healthy elderly volunteers: initial findings at 3.0 Tesla. *Acad Radiol* 15: 776–785, 2008.
35. **Patterson RP, Zhang J.** Evaluation of an EIT reconstruction algorithm using finite difference human thorax models as phantoms. *Physiol Meas* 24: 467–475, 2003.
36. **Pulletz S, Elke G, Zick G, Schadler D, Scholz J, Weiler N, Frerichs I.** Performance of electrical impedance tomography in detecting regional tidal volumes during one-lung ventilation. *Acta Anaesthesiol Scand* 52: 1131–1139, 2008.
37. **Pulletz S, van Genderingen HR, Schmitz G, Zick G, Schadler D, Scholz J, Weiler N, Frerichs I.** Comparison of different methods to define regions of interest for evaluation of regional lung ventilation by EIT. *Physiol Meas* 27: S115–127, 2006.
38. **Rabbani KS, Kabir AM.** Studies on the effect of the third dimension on a two-dimensional electrical impedance tomography system. *Clin Phys Physiol Meas* 12: 393–402, 1991.
39. **Reifferscheid F, Elke G, Pulletz S, Gawelczyk B, Lautenschlager I, Steinfath M, Weiler N, Frerichs I.** Regional ventilation distribution determined by electrical impedance tomography: reproducibility and effects of posture and chest plane. *Respirology* 16: 523–531, 2011.
40. **Richard JC, Pouzot C, Gros A, Tourevieille C, Lebars D, Lavenne F, Frerichs I, Guerin C.** Electrical impedance tomography compared to positron emission tomography for the measurement of regional lung ventilation: an experimental study. *Crit Care* 13: R82, 2009.
41. **Riedel T, Kyburz M, Latzin P, Thamrin C, Frey U.** Regional and overall ventilation inhomogeneities in preterm and term-born infants. *Intensive Care Med* 35: 144–151, 2009.
42. **Rigaud B, Morucci JP.** Bioelectrical impedance techniques in medicine. Part III: Impedance imaging First section: general concepts and hardware. *Crit Rev Biomed Eng* 24: 467–597, 1996.
43. **Robertson HT, Glenny RW, Stanford D, McInnes LM, Luchtel DL, Covert D.** High-resolution maps of regional ventilation utilizing inhaled fluorescent microspheres. *J Appl Physiol* 82: 943–953, 1997.
44. **Rossi A, Ganassini A, Tantucci C, Grassi V.** Aging and the respiratory system. *Aging* 8: 143–161, 1996.
45. **Seagar AD, Brown BH.** Limitations in hardware design in impedance imaging. *Clin Phys Physiol Meas* 8, Suppl A: 85–90, 1987.
46. **Serrano RE, Riu PJ, de Lema B, Casan P.** Assessment of the unilateral pulmonary function by means of electrical impedance tomography using a reduced electrode set. *Physiol Meas* 25: 803–813, 2004.
47. **Steinmann D, Stahl CA, Minner J, Schumann S, Loop T, Kirschbaum A, Priebe HJ, Guttmann J.** Electrical impedance tomography to confirm correct placement of double-lumen tube: a feasibility study. *Br J Anaesth* 101: 411–418, 2008.
48. **van Beek EJ, Dahmen AM, Stavngaard T, Gast KK, Heussel CP, Krummenauer F, Schmiedeskamp J, Wild JM, Sogaard LV, Morbach AE, Schreiber LM, Kauczor HU.** Hyperpolarised 3He MRI versus HRCT in COPD and normal volunteers: PHIL trial. *Eur Respir J* 34: 1311–1321, 2009.
49. **Victorino JA, Borges JB, Okamoto VN, Matos GF, Tucci MR, Caramez MP, Tanaka H, Sipmann FS, Santos DC, Barbas CS, Carvalho CR, Amato MB.** Imbalances in regional lung ventilation: a validation study on electrical impedance tomography. *Am J Respir Crit Care Med* 169: 791–800, 2004.
50. **Wolf GK, Grychtol B, Frerichs I, van Genderingen HR, Zurakowski D, Thompson JE, Arnold JH.** Regional lung volume changes in children with acute respiratory distress syndrome during a derecruitment maneuver. *Crit Care Med* 35: 1972–1978, 2007.
51. **Wrigge H, Zinserling J, Muders T, Varelmann D, Gunther U, von der Groeben C, Magnusson A, Hedenstierna G, Putensen C.** Electrical impedance tomography compared with thoracic computed tomography during a slow inflation maneuver in experimental models of lung injury. *Crit Care Med* 36: 903–909, 2008.
52. **Xu J, Moonen M, Johansson A, Gustafsson A, Bake B.** Quantitative analysis of inhomogeneity in ventilation SPET. *Eur J Nucl Med* 28: 1795–1800, 2001.
53. **Zhao Z, Steinmann D, Frerichs I, Guttmann J, Moller K.** PEEP titration guided by ventilation homogeneity: a feasibility study using electrical impedance tomography. *Crit Care* 14: R8, 2010.